pISSN 1738-2696 · eISSN 2212-5469
https://doi.org/10.1007/s13770-016-0133-8
SPECIAL ISSUE – REVIEW ARTICLE

TERM

Three-Dimensional Cell-Based Bioprinting for Soft Tissue Regeneration

Ji Hyun Kim, James J. Yoo, Sang Jin Lee*

Wake Forest Institute for Regenerative Medicine, Wake Forest School of Medicine, Winston-Salem, NC, USA

Three-dimensional (3D) bioprinting technologies have been developed to offer construction of biological tissue constructs that mimic the anatomical and functional features of native tissues or organs. These cutting-edge technologies could make it possible to precisely place multiple cell types and biomaterials in a single 3D tissue construct. Hence, 3D bioprinting is one of the most attractive and powerful tools to provide more anatomical and functional similarity of human tissues or organs in tissue engineering and regenerative medicine. In recent years, this 3D bioprinting continually shows promise for building complex soft tissue constructs through placement of cell-laden hydrogel-based bioinks in a layer-by-layer fashion. This review will discuss bioprinting technologies and their applications in soft tissue regeneration.

Tissue Eng Regen Med 2016;13(6):647-662

Key Words: Bioprinting; Soft tissue; Hydrogel; Bioinks; Regeneration; Tissue engineering

INTRODUCTION

Tissue engineering and regenerative medicine aim to meet the demand for replacement of tissues or organs. In the last decade, there are various advanced technologies which are producing remarkable success outcomes in the field [1,2]. Among these, three-dimensional (3D) bioprinting technologies for fabricating tissue constructs are a most advanced technique that has potential to accelerate the clinical translation, because these technologies are continually demonstrating the feasibility of building complex tissue constructs at sizes and shapes, which can be anatomically and clinically applicable [3-5]. Through spatial combinations of tissue-specific cell types and biomaterial scaffolds in 3D architecture, we can better harness the reconstructive capability and thereby generate required functions of tissue constructs. In this review we present the strategy of 3D bioprinting for soft tissue regeneration combined with tissue-specific cell types and various hydrogel-based bioinks. Current efforts in 3D bioprinting are focused on the development of the bioinks which can provide mechanical support, cell-specific microenvironmental cues, and negligible cytotoxicity. Advances in the field of suitable cell-compatible bioink materials are necessary for the long-term success of 3D bioprinting technology.

Received: September 29, 2016
Revised: October 31, 2016
Accepted: November 4, 2016
***Corresponding author:** Sang Jin Lee, Wake Forest Institute for Regenerative Medicine, Wake Forest School of Medicine, Medical Center Boulevard, Winston-Salem, NC 27157, USA.
Tel: 1-336-713-7288, Fax: 1-336-713-7290, E-mail: sjlee@wakehealth.edu

BIOPRINTING METHODS FOR CELL PRINTING

Various types of 3D printing methods have been developed for the purpose of cell printing (Table 1). The dimensions of the printing nozzle allow micro-scaled control over the volume and the position of the dispensed patterns containing live cells. Thus, the geometry and composition of the printed structure can be controlled to provide more anatomical and functional similarity to human tissues or organs. In order to print live cells, hydrogel-based bioinks have been used as a carrier material of cells in 3D bioprinting. The choice of bioinks is dependent on the three common printing methods; jetting, laser-induced forward transfer (LIFT), and extrusion-based printing. Each method involves specific characteristics of bioinks for cell printing. The selection of hydrogels as bioink materials is mainly subject to their physicochemical properties under the 3D bioprinting process [6]. The major physiochemical properties of hydrogel-based bioinks can be determined by their rheological properties and crosslinking mechanism which reflect "printability". Various printing and rapid prototyping technologies have been adapted for use in 3D bioprinting strategy.

Table 1. 3D bioprinting technologies for soft tissue regeneration

Tissue/organ	Testing model	Printing method	Cell type	Bioink	Construct dimension	Outcomes	Ref.
Skin	Mouse full-thickness wound	Extrusion	Keratinocytes, fibroblasts	Collagen	5×5 mm^2 (4 layers)	Multi-layered skin constructs with effective proliferation and migration of keratinocytes and fibroblasts	[31]
	Mouse full-thickness wound	Extrusion	AFSCs	Fibrin/collagen	2×2 cm^2	*In situ* skin printing of full-thickness wound closure with vascularization	[33]
	Mouse full-thickness wound	LIFT	Keratinocyte, fibroblasts	Collagen	10×10×2 mm^3	Multi-layered epidermis tissue construction	[4, 32]
	Mouse full-thickness wound	Jetting	Keratinocyte, fibroblasts, ECs	Collagen	17×17 mm^2	Microvasculature in a bilayer skin graft, resulting in improved wound contraction	[68]
	In vitro skin model	Extrusion	Keratinocyte, fibroblasts	Collagen	10×10 mm^2	Dermal/epidermal-like distinctive layers	[19]
	In vitro skin model	Jetting	Keratinocytes, fibroblasts	Collagen	6×6 mm^2	Dermis and epidermis layers	[20]
Adipose tissue	Mouse subcutaneous implantation	Extrusion	ADSCs	Decellularized adipose tissue matrix, PCL	10 (D)× 5 mm (H)	Precisely-defined and flexible dome-shape structure and adipose tissue formation *in vivo*	[34]
Skeletal muscle	Rat ectopic implantation	Extrusion	C2C12 myoblasts	Fibrin	15×5×1 mm^3	Myotybes formation with high alignment	[3]
	In vitro	LIFT+ manual seeding	C2C12 myoblasts	PEGDA fibrin/collagen/ matrigel	6×2 mm^2	Force production and locomotion of muscle strip	[69]
Tendon	*In vitro*	Jetting	Tenocytes	PCL	2 mm (ID) and 3 cm (L)	Increase in cellular metabolism, cell alignment, and collagen type I expression	[38]
Muscle-tendon	*In vitro*	Extrusion	C2C12 myoblasts, NHC/3T3 fibroblasts	Fibrin, PU, PCL	20×5×1 mm^3	Elastic on muscle and stiff on tendon side, >80% cell viability at day 1, MTJ development	[39]
	In vitro	Jetting+ manual seeding	C2C12 myoblasts, C3H10T1/2	PU	-	Biomimetic, sub-micron scaffold patterned with growth factors to modulate spatial control cell fate and alignment	[70]

Table 1. 3D bioprinting technologies for soft tissue regeneration (continued)

Tissue/organ	Testing model	Printing method	Cell type	Bioink	Construct dimension	Outcomes	Ref.
Nerve	Rat sciatic nerve injury	Extrusion	Schwann cells, MSCs	-	2 mm (ID)×1 cm (L)	Three-channel nerve graft construct	[42, 71]
	In vitro	Jetting	Hippocampal and cortical cells, NT2 cells	Fibrin	-	Creation of functional 3D neural sheets with maintenance of neuronal phenotypes	[72]
	In vitro	Jetting	Neural stem cells (C17.2)	Collagen, VEGF-fibrin	-	>92% cell viability after printing	[73]
	Rat sciatic nerve injury	Extrusion	Embryonic sensory neurons, Schwann cells	GelMa+GDNF or NGF	12 mm (L)	A custom Y-shaped nerve conduit containing bifurcating sensory and motor nerve pathways	[74]
	Mouse common fibular nerve injury	LIFT	-	PEG	1 mm (ID) and 5 mm (L)	Neuronal growth and differentiation *in vitro* and organization of regenerated axon paths *in vivo*	[75]
Vessel	*In vitro*	Extrusion	ECs, SMCs, fibroblasts	-	0.9 mm (ID) and 10 cm (L)	Perfused and matured vascular grafts	[42, 43]
	In vitro	Jetting	HUVECs	Gelatin	0.7–1.5 mm (L) ×0.5–1.2 mm (ID)	Perfused functional vascular channels	[76]
	In vitro	Extrusion	Fibroblasts, HUVECs	Pluronic F127, GelMa	3 mm thick	Vascularized heterogeneous tissue constructs	[5]
	In vitro	Extrusion	MSCs, fibroblasts HUVECs	Gelatin, fibrinogen	<1 cm	Thick vascularized tissue on a perfusion chip	[45]
	Rat abdominal aorta	Extrusion	MSCs	-	1.5 mm (ID)	Remodeling and endothelialization	[44]
	In vitro	Extrusion+ manual seeding	10T1/2, HUVECs	Carbohydrate-glass, ECMs	20×10 mm^2	Cylindrical networks and endothelialization to generate perfused vascular channels	[77]
	In vitro	Extrusion	-	Alginate	-	Vessel-like, perfused microfluidic channels	[78]
	In vitro	Extrusion+ manual seeding	MSCs	Alginate/PVA	7×7×7 mm^3	3D hollow fiber scaffolds with microphores on MSC attachment and spreading	[79]

Table 1. 3D bioprinting technologies for soft tissue regeneration (continued)

Tissue/organ	Testing model	Printing method	Cell type	Bioink	Construct dimension	Outcomes	Ref.
Cardiac tissue	Rat myocardial infarction	LIFT	MSCs, HUVECs	PEUU	26×26×1 mm^3	Enhanced blood vessels formation to preserve cardiac function	[46]
	In vitro	Extrusion	Cardiac progenitor cells	Alginate	2×2 cm^2	Homogenous distribution of cells with expression of early cardiac transcription factors	[80]
	In vitro	Jetting	Cardiomyocytes	Alginate	30×8×5 mm^3	Functional cardiac pseudo tissues with contractile function	[10]
	In vitro study	Extrusion	-	Alginate	2.5 cm and 35 mm (L)× 2 mm (D)	3D printed embryonic chick heart and femur bone structure	[47]
Heart valve	*In vitro* study	Extrusion	Aortic root sinus SMCs, aortic VICs	Alginate/gelatin	2 cm wide	Anatomically complex aortic valve conduits	[49]
	In vitro study	Extrusion	Aortic VICs	Me-HA/GelMa	26 mm (D)× 8 mm (H)	Bioprinted trileaflet valve conduits	[50]
	In vitro study	Extrusion+ manual seeding	Aortic valvular interstitial cells	PEGDA, alginate	22 mm (ID)	Heterogeneous aortic valve with valve root and leaflets	[51]
Liver	*In vitro* study	Extrusion	Hepatocytes	Alginate	-	3D liver micro-organ model combined with microfluidics	[58, 59]
	In vitro study	Extrusion	Hepatocytes, stellate cells, ECs	-	1×1 cm^2	Albumin secretion, drug toxicity testing	[81]
	In vitro study	Jetting	hiPSCs	Alginate	-	Hepatocyte-like cells differentiation of iPSCs and albumin secretion	[61]
	In vitro study	Extrusion	ADSCs, hepatocytes	Gelatin/alginate/ fibrin, gelatin/ alginate/chitosan	3.5 cm (D)× 3.5 cm (H)	Mimicry of anatomical liver structure with a vascular-like network and albumin secretion	[82]
	In vitro study	Extrusion	Hepatocytes, HUVECs, lung fibroblasts	PCL, collagen	1×1 cm^2	Vascularized, functional liver structure, albumin secretion and urea synthesis	[83]

Table 1. 3D bioprinting technologies for soft tissue regeneration (continued)

Tissue/organ	Testing model	Printing method	Cell type	Bioink	Construct dimension	Outcomes	Ref.
Brain	*In vitro* study	Jetting	Alveolar epithelial cells, ECs	Matrigel	-	Realistic 3D *in vitro* alveolar model	[62]
	In vitro study	Extrusion	Neural cells	Gellan gum-RGD	1 cm (D)× 1 cm (H)	Bioprinted 3D brain-like structure	[84]
Islet	*In vitro* study	Extrusion	β-cell line/islets	Alginate	2×2 cm^2	Creating porous scaffolds for an extra-hepatic islet delivery system	[63]
Tumor	*In vitro* study	Extrusion	HeLa cells	Gelatin/alginate/ fibrin	10×10×2 mm^3	Cellular spheroid formation	[85]
	In vitro study	Jetting	Ovarian cancer cells, fibroblasts	-	-	Spontaneous multicellular actini formation	[66]

GDNF: glial cell line-derived neurotrophic factor, Me-HA: methacrylated HA, NGF: nerve growth factors, PVA: poly(vinyl alcohol), VICs: valve leaflet interstitial cells, LIFT: laser-induced forward transfer, AFSCs: amniotic fluid-derived stem cells, ECs: endothelial cells, ADSCs: adipose-derived stem cells, MSCs: Mesenchymal stem cells, SMCs: smooth muscle cells, HUVECs: human umbilical vein endothelial cells, hiPSCs: Human induced pluripotent stem cells, PU: polyurethane, GelMa: gelatin methacrylate, PEG: poly(ethylene glycol), PEUU: poly(ester urethane urea), PEGDA: poly(ethylene glycol)diacrylate, PCL: poly(ε-caprolactone), RGD: Arg-Gly-Asp, 3D: three-dimensional, iPSCs: induced pluripotent stem cells, D: diameter, H: height, ID: inner diameter, L: length

Jetting-based printing

Ink-jet printers operate a reservoir that feeds a chamber with extrusion mechanism which forces the bioink with cells through an orifice generating small droplets [7]. Several designs have found success for printing bioinks with biological compounds and/or cells. Common ejection mechanisms are pneumatic-, piezoelectric-, and thermal-based. Pneumatic actuation applies air pressure to the bioinks in concert with a valve regulating the orifice. Piezoelectric ejection chamber has a surface made of a piezoelectric material that deforms with electrical current resulting in a rapid volumetric change forcing bioink out of the chamber through the orifice. Thermal ink-jet system has a chamber with a heating element providing rapid, localized heating to induce bubble formation which propels the bioinks through the orifice. Among these, ink-jet printing method is mostly applied for cell printing. The resolution of the printed patterns using ink-jet printing method is about 20–100 μm [8]. In order to achieve solidification in a desired 3D architecture, the biopaper, layer substrate material, induces solidification of the droplet of bioink [9] or the bioink initiates solidification of the biopaper material [10]. For example, a 3D architecture was fabricated by printing the cell-laden alginate solution (bioink) on calcium chloride solution (biopaper) [9]. On the other hand, the calcium chloride solution (bioink) was printed on the cell-mixed alginate solution (biopaper) [10]. The ink-jet printing method has many advantages, such as high resolution, multiple cartridge option, and low cost; however, a major limitation is that only bioink with low viscosity can be reasonably used for this dispensing method.

Laser-Induced Forward Transfer-based printing

A common LIFT is composed of a pulsed laser source, a target or ribbon coated with a bioink to be transferred, and a receiving substrate. The ribbon is a silicate slide with a metallic absorptive coating. The bioink is evenly loaded on top of the ribbon and oriented face-down above the receiving substrate. High speed laser is focused through the back side of the slide targeting the absorptive layer. Excitation of this absorptive layer produces localized, rapid heating causing bubble formation under the bioink film resulting in a small droplet being ejected from the surface of the ribbon toward the substrate [11]. This method is capable of precisely printing cells with bioinks in relatively small 3D patterns while maintaining cell viability [11]. Major parameters are laser pulse energy and bioink viscosity to control the cell printing process. It has also been used with a wide range of viscosities of bioink materials; however, the process requires rapid gelation mechanism of bioinks to reach high resolution of the printed cell patterns.

Extrusion-based printing

Extrusion-based printing method with micro-scaled nozzle and precise pressure controller or syringe pump is a most common method for cell printing. The cell-laden hydrogel bioinks in the cartridge can be dispensed by controlling pneumatic pressure or piston of the syringe pump. This printing method can construct a composite structure using a multiple-cartridge system capable of dispensing multiple cell types and biomaterials. This printing method offers a relatively wider selection of bioink materials when compared with others. Additionally, biologically active or structural molecules can be incorporated into the bioink. In contrast, extrusion-based printing has comparatively low resolution (50–400 μm). Most of these hydrogel-based printing methods has poor mechanical and structural stability. In this regards, we have recently introduced a novel integrated tissue and organ printing (ITOP) system that deposits cell-laden hydrogel bioinks together with synthetic polymers that impart mechanical strength, there by overcoming current limitations on complexity with structural integrity [3].

HYDROGEL-BASED BIOINKS FOR CELL PRINTING

The required properties of hydrogel-based bioinks are 1) relatively higher viscosity to provide homogenous cell suspension and initial structural integrity, 2) strong shear-thinning behavior to minimize cell damage, and 3) rapid gelation to build a 3D tissue structure. Especially, gelation mechanisms of hydrogels are critical based on the printing process. Various gelation mechanisms have been employed for increasing the stability of 3D hydrogel-based bioinks for cell printing. One approach is the use of thermo-sensitive hydrogels, like gelatin and Pluronic F127, to maintain structure until a crosslinkable bioink is cured for longer periods of hydrogel stability at physiological conditions. This session will review the currently used hydrogels as bioink materials for cell printing. Figure 1 shows a diagram of variables critical to 3D bioprinting strategy.

Alginate

Alginate is a naturally derived anionic polysaccharide exhibiting gelation in the presence of bivalent ions such as Ca^{2+} [12]. This hydrogel has served as a cell delivery material for many tissue engineering applications due to ease of preparation and relatively good cell compatibility; however, the primary drawback the lack of mammalian enzymatic degradation, which limits tissue remodeling when implanted. Also, there is inadequate cell attachment to alginate chains without chemical modification [13]. In the early stage of cell printing, a jetting printing set up was modified for 3D printing by printing of a Ca^{2+}solution into a reservoir of cardiac cells mixed with alginate solution [10]. The printing of the calcium chloride solution induced gelation to form a hollow shell structure in the desired pattern with each shell having an average outer diameter of 25 μm. An elevator system moved the gelled construct down to expose fresh alginate solution to the printed solution to allow formation of a 3D structure in the shape of a two-chambered heart-like structure. The final printed construct demonstrated both cardiac cell beating.

It has been reported that the LIFT printing of multiple skin cell types using alginate to hold the cells in place for patterning on Matrigel-coated substrate was performed successfully [14]. Keratinocytes, fibroblasts, and human adipose-derived stem cells (ADSCs) were printed and assessed for viability, proliferation, apoptosis, and DNA damage. Results indicated over 98% cell viability, proliferation of each cell type, and no significant increase in apoptosis or DNA damage. This study has validated the printing method and the hydrogel carrier for safe patterning of multiple cell types. Another group showed that the LIFT printing system could be combined with other 3D fabrication techniques by printing alginate-based bioink into a poly(ethylene glycol)-diacrylate (PEG-DA) scaffold fabricated by stereolithography [15]. A highly porous scaffold was designed to take the printed bioink structure and had a doughnut shape

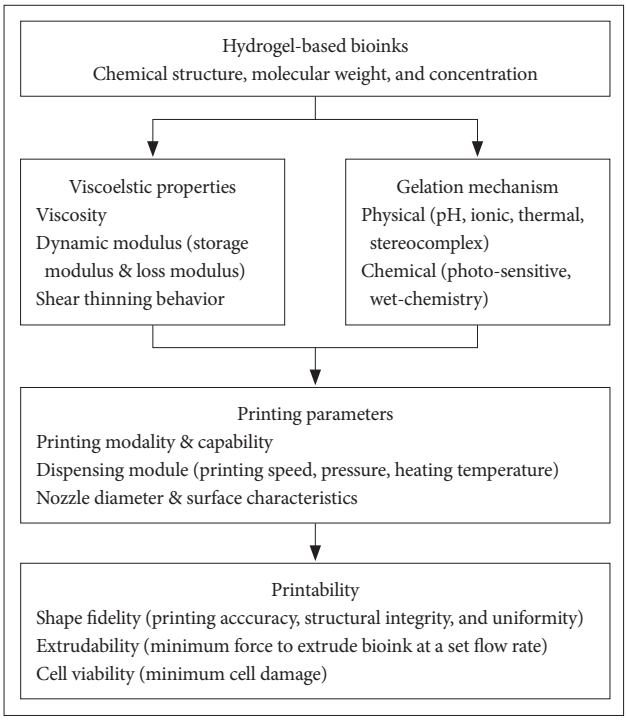

Figure 1. Schematic diagram of variables critical to 3D bioprinting strategy. The hydrogel-based bioinks determine the viscosity, gelation mechanism, and printing parameters, eventually, bioprinted tissue constructs. 3D: three-dimensional.

for engineering a vascular graft. In printing process, two bioinks were prepared: endothelial cells (ECs) in alginate and vascular smooth muscle cells (SMCs) in alginate. The LIFT printing was utilized to position each cell-type into the designed areas of the scaffold to form an EC layer ensheathed by multilayered SMCs. Results stated that the ability of the LIFT printing to safely deposit multiple cells into determined regions of an arbitrary substrate (Fig. 2A, B, and C).

Hyaluronic acid

HA is a glycosaminoglycan found in most of tissues in the body, especially, skin, vitreous humor, and synovial fluid. The high molecular weight and large amount of branching of HA allow for intermolecular hydrogen bonding and high viscosity. Similar to other polysaccharides, HA supports the cell viability, but has low binding motifs in cell attachment. HA has been utilized by the addition of PEG-based arms for crosslinking by photoinitiated acrylate polymerization [16]. Four-armed PEG linkers were used for chemical modification to form TetraPAc crosslinker molecules. These crosslinkers were reacted with thiolated HA, thiolated carboxymethyl HA (CMHA-S), and thiolated gelatin, Gtn-DTPH, to create a crosslinkable printable bioink to improve the cell attachment. Evaluation was conducted on multiple cell types, including NIH3T3, HepG2, and INT 407 cell lines. It has been demonstrated that crosslinker efficiency was obstructed in the TetraPAc8 hydrogels, so bioprinting experiments were conducted using 4:1 CMHA-S:Gtn-DTPH and 4:1 hydrogel: TetraPAc13 to form a 2% (w/v) hydrogel mixture. NIH3T3 were printed at a cell density of 25×10^6 cells/mL by mixing cell pellet with hydrogel and loading into a microcapillary for printing after crosslinking. The crosslinked hydrogel was dispensed as cylindrical filaments, stacked to form a tubular shape, and covered with agarose to maintain structure and orientation of filaments. Results indicated the maintenance of the cell viability, position, and structural orientation with a lumen for 4 weeks (Fig. 2D, E, and F).

Collagen

Collagen type I is the focus of this section as it is the most commonly used for cell printing. Under the appropriate temperature and pH, a pure collagen solution undergoes gelation to form a gel with properties dependent on its solution concentration. Cells attach to collagen through integrin binding and enzymatically degrade collagenous fibers allowing for cell migration and extracellular matrix (ECM) remodeling. Numerous reactive moieties allow for chemical modification and crosslinking to biological and mechanical properties [13]. Unlike other hydrogels, collagen-based bioinks must be handled with care to prevent premature setting, usually kept below 4–10°C. Roth et al. [17] showed that 1% solution of collagen was printed with

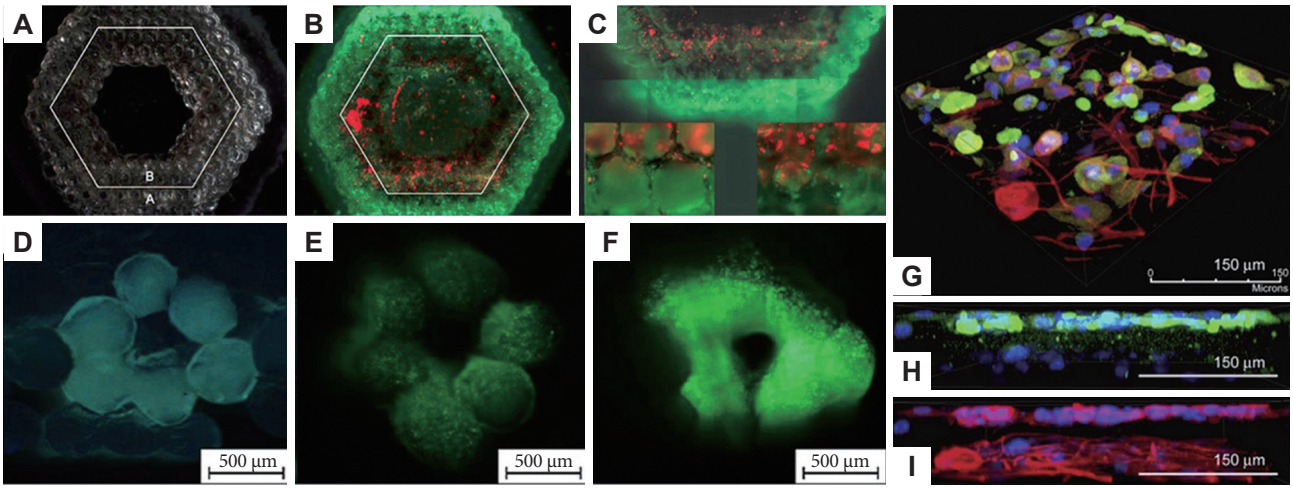

Figure 2. (A, B, and C) Scaffold seeded with cells by means of LIFT. (A) Dark field image. The white hexagon indicates the border between the two scaffold areas seeded with SMCs and ECs, respectively; (B) fluorescence image indicating the location of different cell types after the LIFT procedure; (C) detailed image of the border area. The insets demonstrate that a sharp transition from SMCs to EC-seeded regions is present along the entire thickness of the scaffold. Adapted from Ovsianikov et al. Biofabrication 2010;2:014104, with permission from IOP Publishing [15]. (D) Cross-sectional views of the bioprinted construct taken immediately after printing with encapsulated fluorescent HA-BODIPY tracer for increased visualization. (E) at 14 days, and (F) at 28 days of culture using live/dead staining to highlight viable and dead cells. Green fluorescence indicates calcein AM-stained live cells and red fluorescence indicates ethidium homodimer-1-stained dead cells. Adapted from Skardal et al. Biomaterials 2010;31:6173-6181, with permission from Elsevier [16]. (G, H, and I) Cell images after multilayered printing of fibroblasts and keratinocytes on the tissue culture dish. (G) Volume rendered immunofluorescent images of multilayered printing of keratinocytes and fibroblasts and (H) its projection of keratin-containing keratinocytes layer and (I) β-tubulin-containing keratinocytes and fibroblasts. Adapted from Lee et al. Biomaterials 2009;30:1587-1595, with permission from Elsevier [19]. LIFT: laser-induced forward transfer, SMCs: smooth muscle cells, ECs: endothelial cells, AM: acetoxymethyl, BODIPY: boron-dipyrromethene.

a modified ink-jet printer into the desired patterns on agarose coated glass coverslips. The collagen solution for this approach was kept slightly acidic to prevent clogging. After printing, the collagen hydrogel was dried and reconstituted before cells could be cultured on the patterns. SMC cell line (CRL-1476) were cultured and shown to adhere to and self-align on the collagen patterns. In another approach, Smith et al. [18] performed the printing of aortic ECs using a pneumatically actuated bioplotting system. ECs were mixed with 3 mg/mL of collagen solution titrated to pH 7–7.4, which was subsequently maintained at 10°C. The EC-laden collagen bioink was printed and cultured *in vitro* as printed structure as well as collected for testing the cell viability. The results of the cell viability indicated that cells printed with the small diameter 33-gauge tip had lower viability (46%) than those printed with a 25-gauge tip (86%).

An approach for printing collagen and cells from separate nozzles using an ink-jetting micro-valve dispensing method was performed [19]. The collagen solution at 2 mg/mL was remained acidic and chilled during the printing process. For skin printing, layers of collagen-based bioink were printed, and then treated with aerosolized sodium bicarbonate ($NaHCO_3$) to buffer the pH towards neutral to induce gelation. Once gelled, another layer of collagen or cells was printed in a layer-by-layer. A layer of fibroblasts was sandwiched between collagen layers, followed by six more layers of collagen, then a sandwiched layer of keratinocytes to fabricate a skin-like structure (Fig. 2G, H, and I). The cell viability showed no significant difference between printed construct and control at 1 day after printing for both keratinocytes and fibroblasts. Immunohistochemical staining with pan-keratin and β-tubulin antibodies showed separation of cellular layers with β-tubulin staining throughout, but keratin staining was limited to the top layer of keratinocytes. This demonstrates the survival of cells and spatial control of the printing approach which is needed to offer a functional skin replacement. Another approach using collagen solution with cell suspension to print layered skin-like structure [20]. The micro-nozzle system was set to dispense droplets of chilled, acidic collagen solution that formed a sheet, then aerosolized sodium bicarbonate was sprayed on the surface to induce gelation. Subsequent layers were printed in a similar fashion such that 3 layers of fibroblasts were separated by 2 collagen layers and the structure was capped by 2 layers of keratinocytes. A range of cell densities and droplet spacing distances were tested in an attempt to maximize cell viability. The results of this optimization allowed selecting printing parameters that reflected average cell distribution found in the epidermis and dermis of normal skin (2×10^6 fibroblasts/mL and 5×10^6 keratinocytes/mL with droplets spaced 500 μm).

Gelatin

Gelatin, which is thermally denatured collagen, forms a thermo-reversible hydrogel with strength dependent on concentration. LIFT approach was utilized to print arrays of droplets with embryonic stem cells (ESCs) [21]. The ribbon was coated with 20% (w/v) gelatin solution, then an ESC suspension of $2–5\times10^6$ cells was placed on the gelatin coating. Excess fluid was removed such that the ESCs were partially incorporated and faced down over the receiving substrate during printing. The receiving substrate was coated with 10% gelatin solution to allow printing droplets. The printed patterns showed proliferation and embryoid body formation after 7 days in culture, indicating the printing of ESCs was able to maintain their phenotype and vitality as confirmed by immunostaining for OCT4, nestin, Myf-5, and PDX-1.

Chemical modification of gelatin can be made to enhance crosslinking and bioactivity. It has been reported the use of gelatin methacrylate (GelMa) for printing a complex architecture containing cells and vasculature [5]. Human dermal fibroblasts and 10T1/2 fibroblasts were mixed with GelMa bioink composed of 15% (w/v) GelMa, DMEM:EGM-2 medium, and 0.3 wt% irgacure 2959 photoinitiator. Aqueous 40% (w/v) Pluronic F127 was used as a sacrificial bioink to generate printed paths with open micro-channel for vascular structure. In printing, cell-laden GelMa and sacrificial Pluronic F127 were dispensed and embedded within the GelMa block in predetermined 3D structure. After then, the printed structure was exposed to a UV illumination to induce photo-crosslinking of the GelMa. The temperature was reduced below 4°C to remove Pluronic F127 by the phase transition to create open channels within the GelMa block. A suspension of 1×10^7 human umbilical vein endothelial cells (HUVECs) per mL was seeded into the open channels. Results showed that this approach allowed for the viable deposition of cells in 3D structure with microvessel-like channels that was covered by ECs for provision of nutrients to surrounding cells. This study demonstrated the feasibility to fabricate vascularized tissue constructs using thermo-reversible hydrogel-based bioinks.

Fibrinogen

Fibrinogen is a glycoprotein that is converted by thrombin into fibrin network self-assembles from the straight chain products [13]. Like collagen, fibrin has many motifs allowing for cell attachment and vulnerability to proteases for remodeling. It has been reported the use of printed, cell-laden thrombin solution onto a fibrinogen-coated substrate, resulting in fibrin patterns containing the cells [22]. This study showed that a 60 mg/mL fibrinogen solution, 50 U/mL thrombin, and 80 mM calcium chloride solution were resulted in the highest resolution and

uniformed fibrin printed patterns. Human ECs were suspended in thrombin/calcium chloride solution, then EC-suspended solution was directly printed onto the fibrinogen-coated substrate. Results showed that the printed pattern was cellularized with confluent ECs after 21 days in culture for the endothelium formation in the 3D structure.

Fibrinogen-based bioink has also been used for a 3D multicellular array using LIFT-based printing process [23]. In order to stabilize the viscosity, HA was added to fibrinogen solution to print cell arrays. Endothelial colony-forming cells (ECFCs) were printed along with ASCs in 3D structures such that a 9×9 array of ASC droplets were printed followed by an inset 8×8 array of ECFCs. These droplet arrays were printed onto a layer of fibrinogen-HA which was spray-treated with thrombin/calcium chloride solution to induce the fibrin formation. The cell-laden droplets were converted to fibrin-HA as they encountered the treated substrate with residual thrombin solution. Results showed that ASCs initially migrated towards ECFCs without evidence of ECFC sprouting or migrating at all. Once ASCs contacted the ECFC aggregates, an explosion of ECFC network sprouts began to extend from the initial droplet position and remained as stable networks for several weeks.

Tissue-derived extracellular matrices

ECM is a network of proteins, glycosaminoglycans (GAGs), and other bioactive molecules produced by cells, which supports the function of cells within a tissue. It has been well-known that every tissue has a specific ECM composition suited to the functional needs of the tissue and metabolic needs of the cells. The approaches combined with decellularized ECM and tissue-specific cell type have been shown to be valuable for recapitulating anticipated tissue features [24]. Based on the current finding, tissue-specific ECM-based bioinks derived from decellularized tissues have been developed and examined. Technically, ECM obtained from decellularized tissues can be pulverized and solubilized as a bioink [25]. Rat myoblasts were printed with heart-derived ECM bioink to improve the cardiac tissue formation. ASCs were printed with adipose-derived ECM bioink, followed by adipogenic medium culture to induce adipogenic differentiation. Mesenchymal stem cells (MSCs) isolated from inferior turbinate were printed with cartilage-derived ECM bioink, followed by chondrogenic culture to induce chondrogenic differentiation. Results demonstrates that these tissue-specific ECM-based bioinks are capable of providing crucial cues for target cells engraftment, survival, and tissue formation.

Matrigel is the ECMs derived from murine Engelbreth-Holm-Swarm tumors, which mainly consists of a basement membrane-like material rich in laminin, collagen type IV, and heparan sulfated proteoglycan [26]. Matrigel provides a rich matrix with growth factors and cytokines that support the cellular activities of various cell types as well as the undifferentiated stem cells [27]. Several reports showed the use of Matrigel-based bioinks to print micro-vasculature structures. An approached showed that stem cells with branch patterns of human vascular ECs and SMCs were printed onto Matrigel-coated substrate [28]. HUVECs formed endothelium-like structure in the printed pattern and also connected in patterns similar to the veins of a leaf, while SMCs did not show the same propensity for interconnection. Printed patterns of ECs were covered with SMCs which seem to migrate to the EC pattern and proliferate. Another approach conducted a similar printing experiment using HUVECs from a bioink composed of 0.125% methylcellulose in medium, then collected on a Matrigel-coated or uncoated poly(lactide-co-glycolide) (PLGA) biopaper [29]. Results showed that the printing patterns of HUVECs were well-survived and maintained the printed patterns on Matrigel-coating biopaper, while conforming more to the topography of the thin or uncoated biopaper. Biopaper with printed HUVECs were then stacked to form a vascular network in a thick tissue construct.

CURRENT APPLICATIONS FOR SOFT TISSUE BIOPRINTING

Skin bioprinting

The skin has three layers consisted of epidermis, dermis, and hypodermis, and each layer is composed of different cell types [30]. Several studies have aimed to mimic this complex and multi-layered architecture using skin bioprinting strategy. Researchers have developed engineered skin tissue constructs composed of epidermis and dermis by bioprinting layers of fibroblasts- and keratinocytes-laden collagen hydrogels and these bioprinted skin tissue constructs have been used as *in vitro* skin models. For instance, a 3D human skin tissue construct were fabricated by using inkjet printing method, showing that biologically comparable human skin tissue printing could be possible [20]. In addition, they created a 3D human skin wound model to investigate the feasibility using printing multi-layered skin tissues on a non-planner PDMS surface [19]. A study applied multi-layered, bioprinted skin tissue constructs for *in vivo* skin regeneration. A bioprinted skin construct having 1 layer of fibroblasts-laden collagen matrix as a dermis and 3 layers of keratinocytes-laden collagen matrices as an epidermis was fabrication by the extrusion printing method [31]. The bioprinted skin construct was transplanted in a full-thickness skin excision model of mice. In another study, a cellularized skin construct composed of 20 layers each of fibroblast- and keratinocyte-laden collagen hydrogels on a commercialized acellular

skin graft (Matriderm®, MedSkin Solutions Dr. Suwelack AG, Billerbeck, Germany; 2.3×2.3 cm) was produced by LIFT method [32]. This bioprinted skin construct showed proper cell proliferation and differentiation and skin-like tissue formation in the full-thickness skin wounds of mice [4].

In 2012, *in situ* 3D bioprinting approach has been applied for regeneration of large-scale skin wounds and burns in mice. Results showed that *in situ* skin bioprinting enabled to uniform and direct cover the wound region with cell-laden hydrogels [33]. In order for *in situ* bioprinting, laser scanning of the wound site was performed to obtain information of wound-specific geometry. Then, multi-layered skin constructs composed of amniotic fluid-derived stem cells (AFSCs)-laden fibrin/collagen hydrogels were directly bioprinted onto the wound site. After 2 weeks, re-epithelialization and neovascularization were observed. In this study, advanced scanning system combined with the skin bioprinter enabled to obtain topography and dimensions of human-scale, complex wounds. Moreover, multiple-dispensing modules enabled to bioprint several types of cells and bioinks in layers to approximate the anatomic skin configuration.

Adipose tissue bioprinting

Adipose tissue constructs which had precisely-defined and flexible dome-shape structure were fabricated for reconstructing soft tissues [34]. This adipose tissue construct was engineered by extraction-based printing of human adipose tissue-derived stem cells-laden decellularized adipose tissue matrix-based bioink. The *in vitro* study showed the cells were viable over 2 weeks in culture with expression of standard adipogenic genes. When the adipose tissue constructs were implanted subcutaneously in mice, connective tissue remodeling and adipose tissue formation were observed.

Skeletal muscle bioprinting

Skeletal muscle comprises approximately 40% of the human body weight [35], which is composed of highly aligned muscle fibers. This organization of skeletal muscle is essential for muscle contraction and force generation [36]. Hence, many researchers attempted to mimic the native tissue organization to develop an engineered skeletal muscle construct. Because of 3D bioprinting technology enables to control spatial organization of

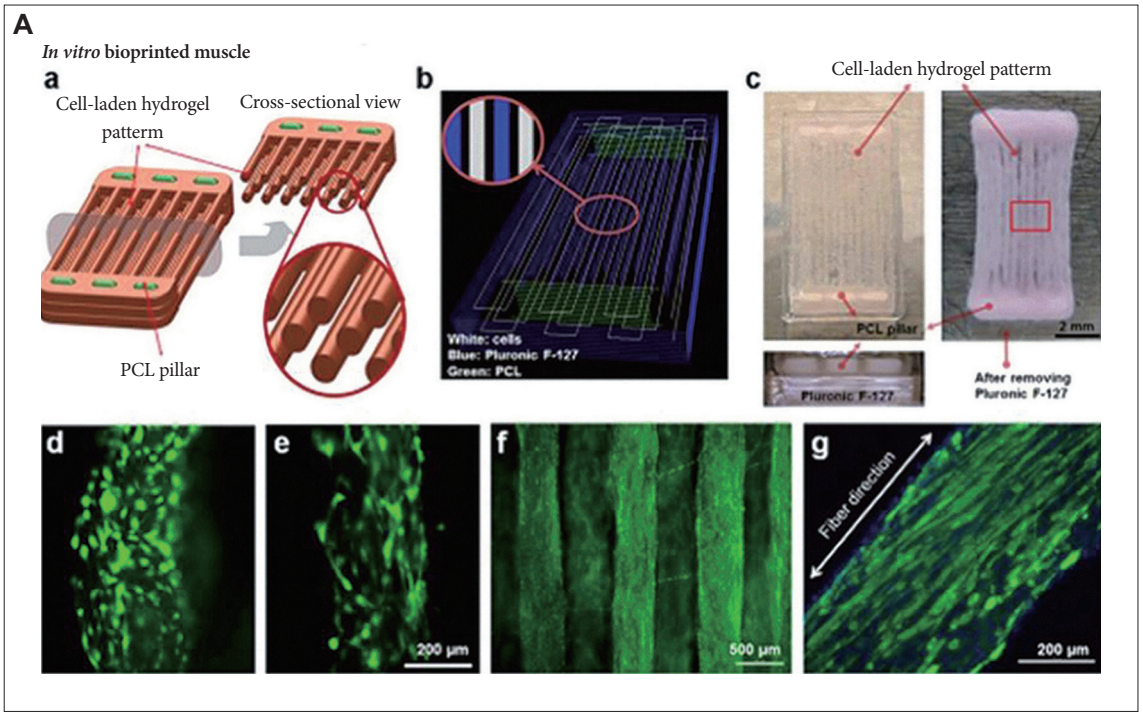

Figure 3. 3D bioprinted skeletal muscle. (A) *In vitro* bioprinted muscle: (a) Designed fiber bundle structure for muscle organization. PCL pillars (green) were used to maintain the structure and to induce the compaction phenomenon for cell alignment. (b) Visualized motion program. (c) 3D patterning outcome (left) before and (after) removing the sacrificial material (d and e). The PCL pillar structure is essential to stabilize the 3D printed muscle and to induce a compaction phenomenon of the cell-laden hydrogel that causes cell alignment in a longitudinal direction of the printed constructs; (d) without and (e) with PCL pillar. The cells with PCL pillar showed unidirectionally organized cellular morphologies that are consistently aligned along the longitudinal axis of the printed construct, which is in contrast to the randomly oriented cellular morphologies without PCL pillar. (f) The live/dead staining indicates high cell viability after the printing process. (g) Immunofluorescent staining for MHC of the 3D printed muscle after 7-day differentiation. Adapted from Kang et al. Nat Biotechnol 2016;34:312-319, with permission from Springer Nature [3]. 3D: three-dimensional, PCL: poly(ε-caprolactone), MHC: myosin heavy chain.

cells and biomaterials in a single architecture, we have recently fabricated an engineered skeletal muscle constructs, consisting of highly oriented muscle-like bundles [3]. In order to engineer this construct with structural integrity, we utilized the ITOP system that could concurrently print multiple cell types and biomaterials in a single tissue construct. At day 3 in growth medium, the printed cells began stretching along the longitudinal axis of the tissue construct, and the constructs underwent compaction from polymeric pillars, keeping the fibers taut during differentiation. After 7 days in differentiation medium, aligned muscle fiber-like structures were observed. Moreover, this bioprinted skeletal muscle construct showed the tissue maturation and host nerve integration in rats (Fig. 3). Results demonstrates that the 3D bioprinting is capable to produce promising structural and functional characteristics *in vitro* and *in vivo*.

Tendon bioprinting

Tendon connects muscle to bone, functioning to transmit forces. Normal tendon has a hierarchical architecture and tendon cells are aligned along with dense collagen fibers [37]. In order to mimic the structural characteristics of tendon tissue, an electrohydrodynamic jetting printing [38] was introduced to fabricate a tubular-shape, multilayered tendon scaffold, having high porosity and oriented micrometer-sized poly(ε-caprolactone) (PCL) fibers. The cultured human tenocytes on the bioprinted scaffold showed high cellular alignment, metabolism, and collagen type I expression.

As described above, tendon directly connects muscle. The 3D bioprinting technology is particularly useful for composite tissues such as muscle-tendon. We used our ITOP system to print four different components for the fabrication of a single integrated muscle-tendon unit (MTU) construct [39]. This MTU construct was comprised of mechanically heterogeneous polymeric materials that was elastic (polyurethane) on the muscle side and relatively stiff (PCL) on the tendon side, in addition to having a tissue-specific distribution of cells with C2C12 myoblasts on the muscle side and NIH/3T3 fibroblasts on the tendon side. Results showed that cells were printed with high cell viability and cellular orientation as well as increased musculotendinous junctional gene expression (Fig. 4). It is demonstrated that 3D bioprinting technology enables a 3D heterogeneous tissue construction having region-specific biological and bio-

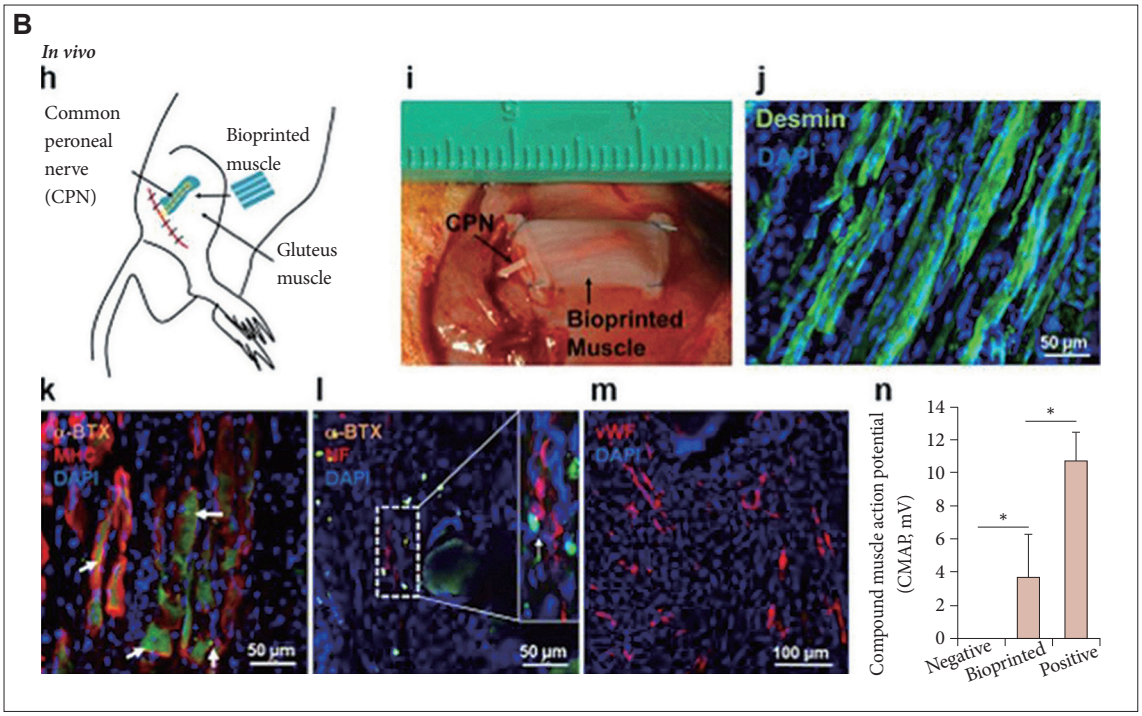

Figure 3. 3D bioprinted skeletal muscle. (B) *In vivo* animal study: (h) Ectopic implantation of bioprinted muscle. (i) The bioprinted muscle was subcutaneously implanted with the CPN embedded, and the harvested at 2 weeks showed presence of organized muscle fibers and innervating capability (α-BTX positive), as confirmed immunostaining using (j) desmin and MHC+and α-BTX+ structure (arrows) in (k). The evidence of nerve integration was demonstrated with double staining of NF+/α-BTX+structure (arrows) in (l). (m) The vascularization was confirmed by vWF immunostaining. (n) Functional assessment of bioprinted muscle constructs at 4 weeks (*p<0.05): positive control: the normal gastrocnemius muscle, negative control: the gluteus muscle after dissected CPN. Adapted from Kang et al. Nat Biotechnol 2016;34:312-319, with permission from Springer Nature [3]. 3D: three-dimensional, MHC: myosin heavy chain, α-BTX: alpha-Bungarotoxin, NF: neurofilament, vWF: von Willebrand factor, PCL: poly(ε-caprolactone), DAPI: 4',6-diamidino-2-phenylindole.

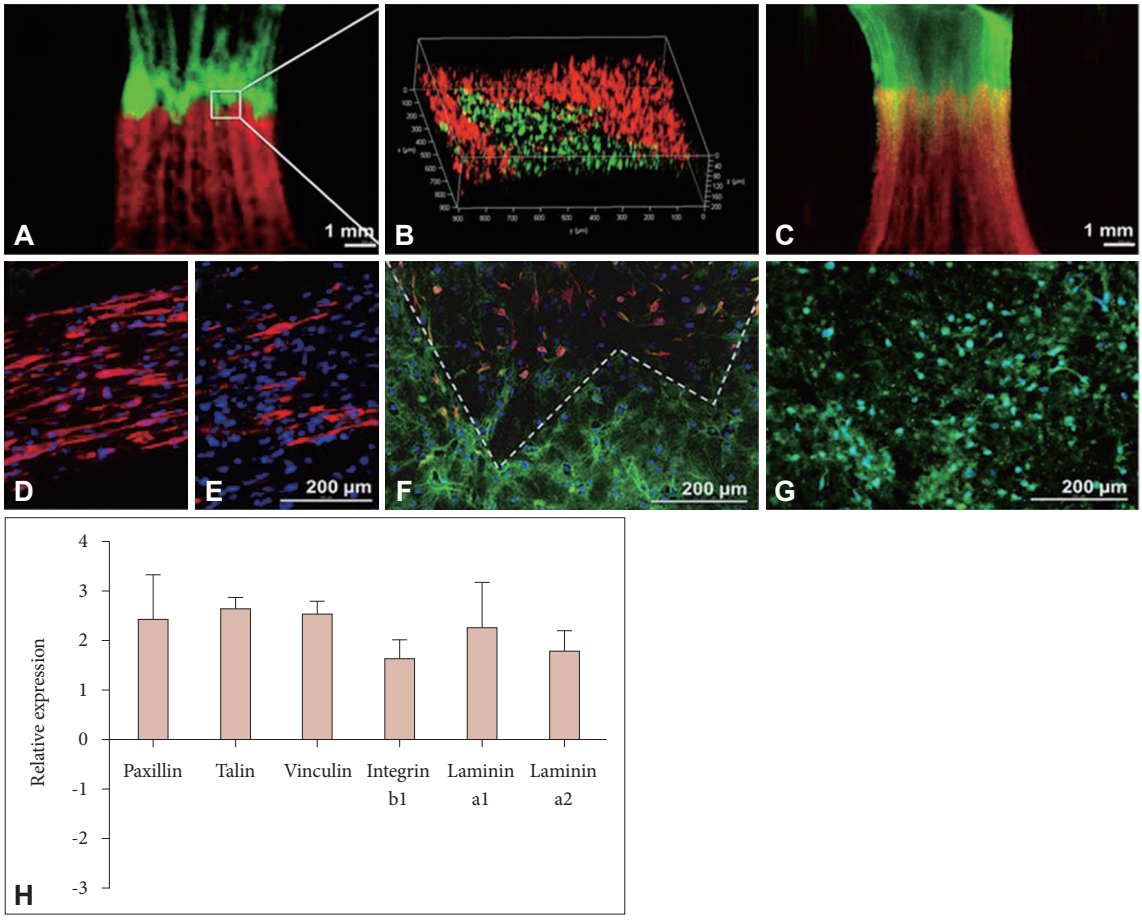

Figure 4. (A, B, and C) Fluorescently-labeled dual-cell printed MTU constructs (green: DiO-labeled C2C12 cells; red: DiI-labeled NIH/3T3 cells; yellow: interface region between green and red fluorescence). (A) Constructs were imaged at (A) 1 day and (C) 7 days in culture to show cell-cell interactions and movement. (B) Confocal microscopic image shows a 3D reconstruction of the interface region on 1 day after printing. (D-G) Immunofluorescence of bioprinted MTU constructs after 7 days in culture. (D and E) On the PU side of the construct, C2C12 cells formed highly-aligned, multinucleated myotube structures [red, (D) desmin and (E) MHC; blue, DAPI]. (F) At the interface region, depicted by the dotted line, differential expression between the two cell types is observed (red, desmin; green, collagen type I; blue, DAPI). (G) On the PCL side of the construct, NIH/3T3 cells secreted collagen type I (green, collagen I; blue, DAPI). (H) Quantitative muscle-tendon junction-associated gene expression profiles of the bioprinted MTU constructs relative to bioprinted muscle-only constructs. Adapted from Merceron et al. Biofabrication 2015;7:035003, with permission from IOP Publishing [39]. MTU: muscle-tendon unit, 3D: three-dimensional, PU: polyurethane, MHC: myosin heavy chain, DAPI: 4',6-diamidino-2-phenylindole, PCL: poly(ε-caprolactone).

mechanical characteristics.

Blood vessels and vascular networks

The incorporation of functional blood vessels or microvascular networks in the engineered tissue constructs is critical for tissue engineering applications [40]. It has been well-known that the limit of oxygen and nutrient diffusion for cell to survival is 100–200 μm [41]. Despite of many efforts to build up vascular networks within 3D tissue constructs, it remains a significant technical challenge. To overcome this limitation, 3D bioprinting technology has been applied to fabricate a functional vascular structure with endothelial cell lining. A scaffold-free bioprinting approach has been applied to fabricate vascular grafts [42,43]. To mimic the native vessel, three types of cell spheroids including human aortic SMCs, human aortic ECs, and human dermal fibroblasts were printed in the agarose templates. These spheroids were self-assembled and formed a cylindrical vascular structure. The resultant scaffold-free vascular structures were biologically matured after 3-week preconditioning by a perfusion bioreactor system. In another study, a scaffold-free tubular vascular tissue was generated using a Bio-3D printer and needle-assay technology [44]. This vascular structure was successfully implanted into abdominal aortas of rats, resulted in tissue remodeling with EC coverage.

In 2016, a 3D cell-laden, vascularized thick tissue (>1 cm) was fabricated by printing a vascular network [45]. Sacrificial Pluronic F127 was printed to create microchannel, then HUVECs were seeded onto luminal surface of the microchannel. The pr-

inted microchannel was integrated with a customized and multicellular perfusion chip composed of human MSCs and human neonatal dermal fibroblasts. This printed microvasculature supported the cell viability and osteogenic differentiation of hMSCs during 6-week in dynamic culture. This study investigated the feasibility of 3D bioprinting technology for developing a physiologically relevant 3D vascularized thick tissue model.

Cardiac tissue bioprinting

Cardiac tissues request a complex anatomy of myocardial organization with contractility, but conventional methods have been limited to fabricate functional cardiac tissue constructs with these requirements. In order to fulfill these requirements, a cardiac patch having geometrically controlled patterns of hMSCs and HUVECs on PEUU was fabricated by a 3D printing method [46]. The bioprinted cardiac patch was implanted to the infarcted hearts in rats and that promoted vascularization and improved cardiac function. Another approach showed a bioprinted half-heart structure containing primary feline adult and H1 cardiomyocytes in alginate hydrogel by a modified jetting printing method [10]. This bioprinted cardiac tissue construct had a porous structure and the printed cells remained their viability in the construct in thickness of 1 cm. Surprisingly, a 3D whole heart construct with internal trabecular structure was developed by a 3D printing technique of freeform reversible embedding of suspended hydrogels (FRESH) [47]. To fabricate the 3D bioprinted whole heart construct, 3D image data (DICOM format) was obtained from an embryonic chick heart to generative a 3D CAD/CAM model. Alginate hydrogel as a bioink was printed within the thermos-reversible support bath consisting of gelatin microparticles at 22°C. After crosslinking, a 3D printed heart construct was released from the gelatin by heating to 37°C. This study demonstrated that the FRESH was able to print the whole heart construct with anatomically complex internal and external architectures.

Heart valve exhibits a 3D complex anatomy containing a valve root and leaflets with a mechanical heterogeneity. To fabricate an anatomically complex, cellularized heart valve, 3D bioprinting technology has been applied [48]. A cellularized heterogeneous valve construct composed of valve root and tri-leaflet was printed by an extrusion-based, dual-nozzle bioprinter [49]. The printed heart valve construct included aortic root sinus SMCs and aortic valve leaflet interstitial cells in alginate/gelatin composite hydrogel based- bioinks. The resultant printed constructs showed high cell viability over 80% with phenotypic retention at 1 week in culture. The design of the heart valve construct was further advanced by improvement of hybrid hydrogel bioink composed of methacrylated HA and GelMa, resulting in a more anatomically accurate, highly viable tri-leaflet valve [50]. For rapid fabrication of anatomical heterogeneous valve structure, a simultaneous 3D printing/photocrosslinking technique has also been introduced [51]. PEG-DA hydrogel-based bioinks with different molecular weights were used to print a heterogeneous aortic valve construct. A UV-LED array was integrated into the deposition tools, so printed hydrogel paths were immediately crosslinked during the printing process. Using this technique, this heterogeneous valve structure was rapidly and accurately fabricated. Furthermore, the cytocompatibility of the cellularized construct was confirmed by closed to 100% cell viability of porcine aortic valvular interstitial cells over 21 days.

Liver bioprinting

In vitro 3D liver models are increasingly interested in drug discovery and toxicity testing due to an important function of liver relating to drug metabolism in the body [52]. Several types of 3D liver models, either normal or diseased, have been developed involving cell-encapsulated hydrogel constructs, cellular spheroids, mini-organs, and microfluidic organs-on-a-chips [53]. However, most *in vitro* models produced by traditional fabrication methods are still unable to deliver a highly controllable, multi-cellular, spatially and functionally complex microscale architecture of the liver [54]. Therefore, 3D bioprinting techniques have been utilize to develop *in vitro* 3D liver models in an accurate, reproducible, and controllable manner. It has been demonstrated that 3D bioprinted liver models offer a platform for deeper understanding of physiological phenomena of the liver and more accurate prediction of drug/toxic responses [54-57]. Another study showed that a 3D liver micro-organ can be fabricated for drug screening and metabolic testing [58]. For a physiologically relevant pharmacokinetic model, a liver micro-organ chamber device was developed by directly printing a hepatocyte-laden alginate hydrogel bioink within the microfluidic chamber. This mini-organ device with continued perfusion flow showed predictable cell viability and proliferation and enhanced liver cell-specific functions confirmed by urea synthesis. Moreover, an enhanced drug metabolic function under the perfused culture conditions was observed compared to the static culture conditions [59]. This study investigated the feasibility using the bioprinted liver micro-organ device for a drug testing model. In order to validate the bioprinted liver constructs, amifostine as a model drug which is an anti-radiation drug was used [60]. This model drug was tested with the printed liver construct composed of epithelial cells and hepatocytes within the microfluidic chamber. The therapeutic effect of amifostine was confirmed with the dual-tissue model, which showed enhanced radioprotective effects, compared to the single tissue model.

Human induced pluripotent stem cells (hiPSCs) was also uti-

lize to bioprint 3D mini-livers [61]. A dual-head valve-based jetting printer was able to print a hiPSCs-laden alginate bioink, while maintaining cell viability and their pluripotency. Moreover, the bioprinted hiPSCs were successfully differentiated into hepatocyte-like cells with hepatocyte markers expression and albumin secretion. This study implies that patient-specific cells can be used for bioprinting tissues or organs for animal-free drug discovery and personalized medicine.

Other soft tissue bioprinting

Lung bioprinting is relatively new, and *in vitro* 3D lung models have been developed for high-throughput screening and drug discovery. To mimic the microenvironment of the native lung, a 3D lung model was fabricated using commercially available extrusion-based bioprinter (BioFactory®, regenHU, Villaz-St-Pierre, Switzerland) [62]. This bioprinted *in vitro* human air-blood barrier model is composed of three layers of ECs, basement membrane, and lung epithelial cells. 3D bioprinting technology facilitated to fabricate very thin and uniform cell-Matrigel layers as a ba-sement membrane, thereby the resultant 3D bioprinted lung model showed physiological and biofunctional resemblance of the native lung.

The FRESH printing method was applied for developing a 3D brain model [47]. The MRI data obtained from human brain was used for bioprinting anatomically-shaped human brain tissues. By introducing the FRESH printing, the 3D printed brain model had complex, external architecture, including the cortex and cerebellum. 3D bioprinting was applied to fabricate an alginate-based scaffold for islet transplantation [63]. The bioprinted extra-hepatic islet delivery system had porous structure to support oxygen and nutrient diffusion. The system included NISIE β-cells, human and mouse islets with high cell viability. When the system was implanted in a subcutaneously in mice, the implanted cells remained their viability and function.

3D bioprinting technologies have been recently applied for *in vitro* cancer research. *In vitro* 3D tumor models using tumor cell spheroids are frequently used for *in vitro* therapeutic screening because the cellular spheroids can provide complex and physiological tumor environments involving cell-cell and cell-matrix interactions [64]. With 3D bioprinting technology, multicellular, controllable and reproducible cell spheroids can be produced. For instance, a 3D cervical tumor model was fabricated by extrusion-printing of HeLa cells derived from cervical cancer tissues [65]. Printed tumor cells in the 3D bioprinted microenvironments were formed into spheroids with higher chemoresistance. A 3D ovarian cancer model with multicellular acini structure consisted of human ovarian cancer cells and normal fibroblasts has been developed for high-throughput screening [66]. Using the jetting printing method, cell density and size of droplets and spatial distance between droplets were precisely controlled. For a breast cancer model, cell spheroids composed of breast cancer cells in the core and breast stromal cells of mammary fibroblasts, ECs and adipose cells were directly printed into multi-well plates for high-throughput screening of chemotherapeutic drugs [67]. These 3D bioprinted cancer models would be an effective tool for development of anti-cancer therapeutics and drug screening.

SUMMARY AND FUTURE DIRECTIONS

3D bioprinting technologies hold great promise to overcome the current limitations in tissue engineering and regenerative medicine. Currently, there has been much effort to develop novel printing mechanisms and hydrogel-based bioinks to achieve high resolution of the constructs. Advanced printing mechanisms may offer increasingly complex designs with anatomical and functional similarity of native tissues. The current jetting-based method using cell-laden hydrogel bioinks has achieved relatively high resolution of approximately 20–100 μm [8]; however, this method has limited to build large tissue constructs with structural integrity. The extrusion-based method has printed the cell-laden hydrogel bioinks down to approximately 50–400 μm in layer thickness [3]; however, the shear stress to the hydrogel bioinks through the nozzle dramatically increases when the nozzle diameter decreases, resulting in high cell damage. On the other hand, a new hydrogel bioink system for cell printing needs to be develop for improving printability with high resolution capability. Availability of currently available hydrogels that can suffice as cell printing bioinks but which also provide tunable mechanical properties, cell-matrix interaction, and negligible cytotoxicity is limited. Advances in the bioprinting of suitable cell-compatible hydrogel-based bioinks are critical for the long-term success of cell printing for soft tissue regeneration.

3D bioprinting technologies are able to construct 3D free-form shapes containing multiple cell types, biomaterials, and bioactive molecules, resulting in sophisticated architectures that have the potential to repair damaged or diseased human tissues and organs. Therefore, 3D bioprinting technologies hold great promise in tissue engineering and regenerative medicine. Even if there is much work to be accomplished to advance these technologies toward successful clinical translation, our efforts will continually contribute to deliver clinically applicable bioengineered tissue constructs until this strategy is able to improve the lives of patients.

Acknowledgements

This review paper was supported by the Armed Forces Insti-

tute of Regenerative Medicine (W81XWH-13-2-0052).

Conflicts of Interest

The authors have no financial conflicts of interest.

Ethical Statement

There are no animal experiments carried out for this article.

REFERENCES

1. Atala A, Kasper FK, Mikos AG. Engineering complex tissues. Sci Transl Med 2012;4:160rv12.
2. Withers GS. New ways to print living cells promise breakthroughs for engineering complex tissues in vitro. Biochem J 2006;394(Pt 2):e1-e2.
3. Kang HW, Lee SJ, Ko IK, Kengla C, Yoo JJ, Atala A. A 3D bioprinting system to produce human-scale tissue constructs with structural integrity. Nat Biotechnol 2016;34:312-319.
4. Michael S, Sorg H, Peck CT, Koch L, Deiwick A, Chichkov B, et al. Tissue engineered skin substitutes created by laser-assisted bioprinting form skin-like structures in the dorsal skin fold chamber in mice. PLoS One 2013;8:e57741.
5. Kolesky DB, Truby RL, Gladman AS, Busbee TA, Homan KA, Lewis JA. 3D bioprinting of vascularized, heterogeneous cell-laden tissue constructs. Adv Mater 2014;26:3124-3130.
6. Malda J, Visser J, Melchels FP, Jüngst T, Hennink WE, Dhert WJ, et al. 25th anniversary article: Engineering hydrogels for biofabrication. Adv Mater 2013;25:5011-5028.
7. Klebe RJ. Cytoscribing: a method for micropositioning cells and the construction of two- and three-dimensional synthetic tissues. Exp Cell Res 1988;179:362-373.
8. Melchels FP, Domingos MA, Klein TJ, Malda J, Bartolo PJ, Hutmacher DW. Additive manufacturing of tissues and organs. Prog Polym Sci 2012;37:1079-1104.
9. Nakamura M, Iwanaga S, Henmi C, Arai K, Nishiyama Y. Biomatrices and biomaterials for future developments of bioprinting and biofabrication. Biofabrication 2010;2:014110.
10. Xu T, Baicu C, Aho M, Zile M, Boland T. Fabrication and characterization of bio-engineered cardiac pseudo tissues. Biofabrication 2009;1:035001.
11. Guillotin B, Guillemot F. Cell patterning technologies for organotypic tissue fabrication. Trends Biotechnol 2011;29:183-190.
12. Jin R, Dijkstra PJ. Hydrogels for tissue engineering applications. In: Ottenbrite RM, Park K, Okano T, editors. Biomedical Applications of Hydrogels Handbook. New York: Springer; 2010. p. 203-221.
13. Nair LS, Laurencin CT. Biodegradable polymers as biomaterials. Pro Polym Sci 2007;32:762-798.
14. Koch L, Kuhn S, Sorg H, Gruene M, Schlie S, Gaebel R, et al. Laser printing of skin cells and human stem cells. Tissue Eng Part C Methods 2010;16:847-854.
15. Ovsianikov A, Gruene M, Pflaum M, Koch L, Maiorana F, Wilhelmi M, et al. Laser printing of cells into 3D scaffolds. Biofabrication 2010;2:014104.
16. Skardal A, Zhang J, Prestwich GD. Bioprinting vessel-like constructs using hyaluronan hydrogels crosslinked with tetrahedral polyethylene glycol tetracrylates. Biomaterials 2010;31:6173-6181.
17. Roth EA, Xu T, Das M, Gregory C, Hickman JJ, Boland T. Inkjet printing for high-throughput cell patterning. Biomaterials 2004;25:3707-3715.
18. Smith CM, Stone AL, Parkhill RL, Stewart RL, Simpkins MW, Kachurin AM, et al. Three-dimensional bioassembly tool for generating viable tissue-engineered constructs. Tissue Eng 2004;10:1566-1576.
19. Lee W, Debasitis JC, Lee VK, Lee JH, Fischer K, Edminster K, et al. Multi-layered culture of human skin fibroblasts and keratinocytes through three-dimensional freeform fabrication. Biomaterials 2009;30:1587-1595.
20. Lee V, Singh G, Trasatti JP, Bjornsson C, Xu X, Tran TN, et al. Design and fabrication of human skin by three-dimensional bioprinting. Tissue Eng Part C Methods 2014;20:473-484.
21. Raof NA, Schiele NR, Xie Y, Chrisey DB, Corr DT. The maintenance of pluripotency following laser direct-write of mouse embryonic stem cells. Biomaterials 2011;32:1802-1808.
22. Cui X, Boland T. Human microvasculature fabrication using thermal inkjet printing technology. Biomaterials 2009;30:6221-6227.
23. Gruene M, Pflaum M, Hess C, Diamantouros S, Schlie S, Deiwick A, et al. Laser printing of three-dimensional multicellular arrays for studies of cell-cell and cell-environment interactions. Tissue Eng Part C Methods 2011;17:973-982.
24. Badylak SF. The extracellular matrix as a scaffold for tissue reconstruction. Semin Cell Dev Biol 2002;13:377-383.
25. Pati F, Jang J, Ha DH, Kim SW, Rhie JW, Shim JH, et al. Printing three-dimensional tissue analogues with decellularized extracellular matrix bioink. Nat Commun 2014;5:3935.
26. Kleinman HK, McGarvey ML, Liotta LA, Robey PG, Tryggvason K, Martin GR. Isolation and characterization of type IV procollagen, laminin, and heparan sulfate proteoglycan from the EHS sarcoma. Biochemistry 1982;21:6188-6193.
27. Hughes CS, Postovit LM, Lajoie GA. Matrigel: a complex protein mixture required for optimal growth of cell culture. Proteomics 2010;10:1886-1890.
28. Wu PK, Ringeisen BR. Development of human umbilical vein endothelial cell (HUVEC) and human umbilical vein smooth muscle cell (HUVSMC) branch/stem structures on hydrogel layers via biological laser printing (BioLP). Biofabrication 2010;2:014111.
29. Pirlo RK, Wu P, Liu J, Ringeisen B. PLGA/hydrogel biopapers as a stackable substrate for printing HUVEC networks via BioLP. Biotechnol Bioeng 2012;109:262-273.
30. Bouwstra JA, Honeywell-Nguyen PL, Gooris GS, Ponec M. Structure of the skin barrier and its modulation by vesicular formulations. Prog Lipid Res 2003;42:1-36.
31. Yoon H, Lee JS, Yim H, Kim G, Chun W. Development of cell-laden 3D scaffolds for efficient engineered skin substitutes by collagen gelation. Rsc Adv 2016;6:21439-21447.
32. Koch L, Deiwick A, Schlie S, Michael S, Gruene M, Coger V, et al. Skin tissue generation by laser cell printing. Biotechnol Bioeng 2012;109:1855-1863.
33. Skardal A, Mack D, Kapetanovic E, Atala A, Jackson JD, Yoo J, et al. Bioprinted amniotic fluid-derived stem cells accelerate healing of large skin wounds. Stem Cells Transl Med 2012;1:792-802.
34. Pati F, Ha DH, Jang J, Han HH, Rhie JW, Cho DW. Biomimetic 3D tissue printing for soft tissue regeneration. Biomaterials 2015;62:164-175.
35. Frontera WR, Ochala J. Skeletal muscle: a brief review of structure and function. Calcif Tissue Int 2015;96:183-195.
36. Ostrovidov S, Hosseini V, Ahadian S, Fujie T, Parthiban SP, Ramalingam M, et al. Skeletal muscle tissue engineering: methods to form skeletal myotubes and their applications. Tissue Eng Part B Rev 2014;20:403-436.
37. Goh JC, Ouyang HW, Toh SL, Lee EH. Tissue engineering techniques in tendon and ligament replacement. Med J Malaysia 2004;59 Suppl B:47-48.
38. Wu Y, Wang Z, Ying Hsi Fuh J, San Wong Y, Wang W, San Thian E. Direct E-jet printing of three-dimensional fibrous scaffold for tendon tissue engineering. J Biomed Mater Res B Appl Biomater 2015 Dec 16 [Epub ahead of print].
39. Merceron TK, Burt M, Seol YJ, Kang HW, Lee SJ, Yoo JJ, et al. A 3D bioprinted complex structure for engineering the muscle-tendon unit. Biofabrication 2015;7:035003.
40. Novosel EC, Kleinhans C, Kluger PJ. Vascularization is the key challenge in tissue engineering. Adv Drug Deliv Rev 2011;63:300-311.
41. Jain RK, Au P, Tam J, Duda DG, Fukumura D. Engineering vascularized tissue. Nat Biotechnol 2005;23:821-823.

42. Marga F, Jakab K, Khatiwala C, Shepherd B, Dorfman S, Hubbard B, et al. Toward engineering functional organ modules by additive manufacturing. Biofabrication 2012;4:022001.
43. Norotte C, Marga FS, Niklason LE, Forgacs G. Scaffold-free vascular tissue engineering using bioprinting. Biomaterials 2009;30:5910-5917.
44. Itoh M, Nakayama K, Noguchi R, Kamohara K, Furukawa K, Uchihashi K, et al. Scaffold-free tubular tissues created by a Bio-3D printer undergo remodeling and endothelialization when implanted in rat aortae. PLoS One 2015;10:e0136681.
45. Kolesky DB, Homan KA, Skylar-Scott MA, Lewis JA. Three-dimensional bioprinting of thick vascularized tissues. Proc Natl Acad Sci U S A 2016;113:3179-3184.
46. Gaebel R, Ma N, Liu J, Guan J, Koch L, Klopsch C, et al. Patterning human stem cells and endothelial cells with laser printing for cardiac regeneration. Biomaterials 2011;32:9218-9230.
47. Hinton TJ, Jallerat Q, Palchesko RN, Park JH, Grodzicki MS, Shue HJ, et al. Three-dimensional printing of complex biological structures by freeform reversible embedding of suspended hydrogels. Sci Adv 2015;1:e1500758.
48. Jana S, Lerman A. Bioprinting a cardiac valve. Biotechnol Adv 2015;33:1503-1521.
49. Duan B, Hockaday LA, Kang KH, Butcher JT. 3D bioprinting of heterogeneous aortic valve conduits with alginate/gelatin hydrogels. J Biomed Mater Res A 2013;101:1255-1264.
50. Duan B, Kapetanovic E, Hockaday LA, Butcher JT. Three-dimensional printed trileaflet valve conduits using biological hydrogels and human valve interstitial cells. Acta Biomater 2014;10:1836-1846.
51. Hockaday LA, Kang KH, Colangelo NW, Cheung PY, Duan B, Malone E, et al. Rapid 3D printing of anatomically accurate and mechanically heterogeneous aortic valve hydrogel scaffolds. Biofabrication 2012;4:035005.
52. Bernal W, Wendon J. Acute liver failure. N Engl J Med 2013;369:2525-2534.
53. Bhatia SN, Ingber DE. Microfluidic organs-on-chips. Nat Biotechnol 2014;32:760-772.
54. Pati F, Gantelius J, Svahn HA. 3D bioprinting of tissue/organ models. Angew Chem Int Ed Engl 2016;55:4650-4665.
55. Mandrycky C, Wang Z, Kim K, Kim DH. 3D bioprinting for engineering complex tissues. Biotechnol Adv 2016;34:422-434.
56. Ozbolat IT, Peng W, Ozbolat V. Application areas of 3D bioprinting. Drug Discov Today 2016;21:1257-1271.
57. Arslan-Yildiz A, El Assal R, Chen P, Guven S, Inci F, Demirci U. Towards artificial tissue models: past, present, and future of 3D bioprinting. Biofabrication 2016;8:014103.
58. Chang R, Nam J, Sun W. Direct cell writing of 3D microorgan for in vitro pharmacokinetic model. Tissue Eng Part C Methods 2008;14:157-166.
59. Chang R, Emami K, Wu H, Sun W. Biofabrication of a three-dimensional liver micro-organ as an in vitro drug metabolism model. Biofabrication 2010;2:045004.
60. Snyder JE, Hamid Q, Wang C, Chang R, Emami K, Wu H, et al. Bioprinting cell-laden matrigel for radioprotection study of liver by pro-drug conversion in a dual-tissue microfluidic chip. Biofabrication 2011; 3:034112.
61. Faulkner-Jones A, Fyfe C, Cornelissen DJ, Gardner J, King J, Courtney A, et al. Bioprinting of human pluripotent stem cells and their directed differentiation into hepatocyte-like cells for the generation of mini-livers in 3D. Biofabrication 2015;7:044102.
62. Horváth L, Umehara Y, Jud C, Blank F, Petri-Fink A, Rothen-Rutishauser B. Engineering an in vitro air-blood barrier by 3D bioprinting. Sci Rep 2015;5:7974.
63. Marchioli G, van Gurp L, van Krieken PP, Stamatialis D, Engelse M, van Blitterswijk CA, et al. Fabrication of three-dimensional bioplotted hydrogel scaffolds for islets of Langerhans transplantation. Biofabrication 2015;7:025009.
64. Weiswald LB, Bellet D, Dangles-Marie V. Spherical cancer models in tumor biology. Neoplasia 2015;17:1-15.
65. Friedrich J, Ebner R, Kunz-Schughart LA. Experimental anti-tumor therapy in 3-D: spheroids--old hat or new challenge? Int J Radiat Biol 2007;83:849-871.
66. Xu F, Celli J, Rizvi I, Moon S, Hasan T, Demirci U. A three-dimensional in vitro ovarian cancer coculture model using a high-throughput cell patterning platform. Biotechnol J 2011;6:204-212.
67. King SM, Presnell SC, Nguyen DG. Development of 3D bioprinted human breast cancer for in vitro drug screening. Cancer Res. 2014;74 (19 suppl):Astract nr 2034.
68. Yanez M, Rincon J, Dones A, De Maria C, Gonzales R, Boland T. In vivo assessment of printed microvasculature in a bilayer skin graft to treat full-thickness wounds. Tissue Eng Part A 2015;21:224-233.
69. Cvetkovic C, Raman R, Chan V, Williams BJ, Tolish M, Bajaj P, et al. Three-dimensionally printed biological machines powered by skeletal muscle. Proc Natl Acad Sci U S A 2014;111:10125-10130.
70. Ker ED, Nain AS, Weiss LE, Wang J, Suhan J, Amon CH, et al. Bioprinting of growth factors onto aligned sub-micron fibrous scaffolds for simultaneous control of cell differentiation and alignment. Biomaterials 2011;32:8097-8107.
71. Owens CM, Marga F, Forgacs G, Heesch CM. Biofabrication and testing of a fully cellular nerve graft. Biofabrication 2013;5:045007.
72. Xu T, Gregory CA, Molnar P, Cui X, Jalota S, Bhaduri SB, et al. Viability and electrophysiology of neural cell structures generated by the inkjet printing method. Biomaterials 2006;27:3580-3588.
73. Lee YB, Polio S, Lee W, Dai G, Menon L, Carroll RS, et al. Bio-printing of collagen and VEGF-releasing fibrin gel scaffolds for neural stem cell culture. Exp Neurol 2010;223:645-652.
74. Johnson BN, Lancaster KZ, Zhen G, He J, Gupta MK, Kong YL, et al. 3D printed anatomical nerve regeneration pathways. Adv Funct Mater 2015;25:6205-6217.
75. Pateman CJ, Harding AJ, Glen A, Taylor CS, Christmas CR, Robinson PP, et al. Nerve guides manufactured from photocurable polymers to aid peripheral nerve repair. Biomaterials 2015;49:77-89.
76. Lee VK, Kim DY, Ngo H, Lee Y, Seo L, Yoo SS, et al. Creating perfused functional vascular channels using 3D bio-printing technology. Biomaterials 2014;35:8092-8102.
77. Miller JS, Stevens KR, Yang MT, Baker BM, Nguyen DH, Cohen DM, et al. Rapid casting of patterned vascular networks for perfusable engineered three-dimensional tissues. Nat Mater 2012;11:768-774.
78. Zhang Y, Yu Y, Ozbolat IT. Direct bioprinting of vessel-like tubular microfluidic channels. J Nanotechnol Eng Med 2013;4:0210011-0210017.
79. Luo Y, Lode A, Gelinsky M. Direct plotting of three-dimensional hollow fiber scaffolds based on concentrated alginate pastes for tissue engineering. Adv Healthc Mater 2013;2:777-783.
80. Gaetani R, Doevendans PA, Metz CH, Alblas J, Messina E, Giacomello A, et al. Cardiac tissue engineering using tissue printing technology and human cardiac progenitor cells. Biomaterials 2012;33:1782-1790.
81. Nguyen DG, Funk J, Robbins JB, Crogan-Grundy C, Presnell SC, Singer T, et al. Bioprinted 3D primary liver tissues allow assessment of organ-level response to clinical drug induced toxicity in vitro. PLoS One 2016;11:e0158674.
82. Li SJ, Xiong Z, Wang XH, Yan YN, Liu HX, Zhang RJ. Direct fabrication of a hybrid cell/hydrogel construct by a double-nozzle assembling technology. J Bioact Compat Pol 2009;24:249-265.
83. Lee JW, Choi YJ, Yong WJ, Pati F, Shim JH, Kang KS, et al. Development of a 3D cell printed construct considering angiogenesis for liver tissue engineering. Biofabrication 2016;8:015007.
84. Lozano R, Stevens L, Thompson BC, Gilmore KJ, Gorkin R 3rd, Stewart EM, et al. 3D printing of layered brain-like structures using peptide modified gellan gum substrates. Biomaterials 2015;67:264-273.
85. Zhao Y, Yao R, Ouyang L, Ding H, Zhang T, Zhang K, et al. Three-dimensional printing of Hela cells for cervical tumor model in vitro. Biofabrication 2014;6:035001.